Research Square

Preprints are preliminary reports that have not undergone peer review.
They should not be considered conclusive, used to inform clinical practice,
or referenced by the media as validated information.

Multiparametric MRI for Early Response Assessment in Early-Stage Breast Cancer Treated with Single-Fraction Neoadjuvant Radiotherapy: A Single-Institution Feasibility Study

Ayyaz Qadir

ayyaz.qadir@monash.edu

Monash Univeristy https://orcid.org/0009-0002-4400-3433

Nabita Singh

Monash Univeristy

Eddie Lau

Austin Health

Mark Tacey

Austin Health

Michael Chao

Austin Health

Sergio Uribe

Monash Univeristy

Farshad Foroudi

Austin Health

Research Article

Keywords: Breast cancer, Neoadjuvant Radiotherapy, Multiparametric MRI, Apparent Diffusion Coefficient, Treatment response

Posted Date: February 25th, 2026

DOI: https://doi.org/10.21203/rs.3.rs-8931170/v1

License: This work is licensed under a Creative Commons Attribution 4.0 International License.
Read Full License

Additional Declarations: The authors declare no competing interests.

Abstract

Purpose

Single-fraction neoadjuvant radiotherapy (SF-NRT) is a promising alternative for patients with low-risk, early-stage breast cancer. However, the optimal post-treatment interval for assessing response remains largely undefined. This study evaluated the feasibility of multiparametric MRI (mp-MRI) for detecting early biological changes after SF-NRT within the arm Magnetic Resonance Image Guided Single Fraction Preoperative Radiotherapy for Early Breast Cancer (RICE) feasibility trial.

Methods

Nine postmenopausal women (median age 69 years) with ER/PR-positive, grade 1–2 invasive ductal carcinoma ≤ 20 mm underwent a single 21 Gy preoperative fraction on the Elekta Unity 1.5 T MR-linac. MRI (1.5 T Philips Ingenia Ambition) was performed at baseline and five weeks post-treatment. Imaging included diffusion-weighted (ADC), standard DCE-MRI with voxel-wise signal enhancement ratio (SER) mapping, and ultrafast DCE analysis. Pathologic response was classified using the modified Miller–Payne system.

Results

Six patients (67%) demonstrated partial pathologic response and three (33%) were non-responders; none achieved pathologic complete response (pCR). Across all patients, ADC increased (0.99×10^{-3} to 1.18×10^{-3} mm^2/s), with partial responders showing greater percentage rises compared to non responders (+ 44.5% vs + 11.1%). SER habitat analysis revealed decreased washout and intermediate-enhancing voxels and a decline in peak SER (0.98 to 0.83), consistent with reduced perfusion heterogeneity. Tumor morphological analysis and ultrafast parameters displayed minimal differences and large inter-patient variability.

Conclusions

mp-MRI demonstrated biologically plausible diffusion and perfusion changes at five weeks following SF-NRT, with directional differences between response groups preceding measurable morphologic regression. These exploratory findings require validation in larger cohorts.

Trial registration

This trial is registered with the Australian New Zealand Clinical Trials Registry (ANZCTR). Registered 31st of May 2021. Registration number: ACTRN12621000659808.

Background

Single-fraction neoadjuvant radiotherapy (SF-NRT) is emerging as a promising treatment option for patients with low-risk, early-stage breast cancer [1–7]. By targeting the intact tumour rather than the postoperative cavity, SF-NRT has the potential to reduce treatment burden and radiation-induced toxicity, thereby improving quality of life. However, despite growing clinical interest, the optimal timing between SF-NRT and surgery remains unclear, with reported timelines ranging from one week to twelve months [2–5,7]. The ability to identify patients who achieve a pathological complete response (pCR) as early as possible could enable more personalised care, allowing surgery to be safely delayed or even omitted in responders, while supporting timely escalation for non-responders.

Magnetic resonance imaging (MRI) has long been used to monitor tumour response during neoadjuvant chemotherapy (NAC), but findings have varied widely due to differences in imaging protocols and analytic methods [8,9]. In clinical practice, response assessment still relies primarily on size-based criteria; however, early morphological changes often lag behind underlying biological alterations in tumour vascularity and cellularity, limiting their value for early response prediction [10–12]. To address these limitations, functional MRI techniques, including multiparametric MRI (mp-MRI), provide a non-invasive means of assessing tumour vascular and microstructural properties that may change early during treatment [10].

At a more granular level, specific quantitative metrics derived from mp-MRI provide biologically interpretable markers of tumour response. The apparent diffusion coefficient (ADC), derived from diffusion-weighted imaging (DWI), reflects the degree of water mobility within tissue and is commonly interpreted as a surrogate of tumour cellularity; increases in ADC following treatment are thought to reflect tumour cell death and expansion of the extracellular space [10,11]. Dynamic contrast-enhanced MRI (DCE-MRI) characterises tumour vascular behaviour through analysis of contrast enhancement kinetics [10]. Voxel-wise metrics such as the signal enhancement ratio (SER) enable classification of enhancing tumour regions into kinetic “habitats” (washout, plateau, and persistent), which are thought to represent areas with differing vascular permeability and contrast clearance properties [13–18]. Ultrafast DCE-MRI extends this approach by capturing the very early phases of contrast arrival with high temporal resolution, generating semi-quantitative parameters sensitive to rapid perfusion dynamics and microvascular permeability[19–22]. Together, these measures provide a biologically grounded framework for probing early treatment-induced vascular and microstructural changes that may precede overt morphological response.

Although mp-MRI has demonstrated prognostic value in the NAC setting [19,23–28], its role in predicting response following SF-NRT remains poorly described. Prior studies [29–31] have shown that MRI signal changes can appear as early as one-week post-treatment, however, these are often dominated by transient inflammatory effects rather than true physiological response. As such, the earliest interval at which genuine treatment-induced changes can be distinguished from acute post-radiation inflammation

remains unknown. To address this gap, we evaluated MRI-derived biomarkers within the RICE trial (Magnetic Resonance Imaging-guided Single-fraction Preoperative Radiotherapy for Early-stage Breast Cancer: Feasibility Study), focusing on early treatment changes observed approximately five weeks post-SF-NRT, a pragmatic interval chosen to balance early response assessment with sufficient time for acute inflammatory effects to subside.

Methods

Study Population and treatment

Details of the RICE trial have been reported previously [32]. Briefly, eligible patients were women aged ≥ 60 years with unifocal, grade 1–2, ER/PR-positive invasive breast carcinoma ≤ 20 mm on imaging, clinically node-negative, and visible on MRI for treatment localisation. Key inclusion and exclusion criteria are summarised in Table 1. All patients provided written informed consent, and the study was approved by the institutional Human Research Ethics Committee.

Table 1
Overview of the inclusion and exclusion criteria for the RICE trial.

Inclusion	Exclusion
Age ≥ 60 years	Previous Radiotherapy to same breast
Unifocal	Suspicious diffuse microcalcifications
Tumor Visible on pre-treatment imaging	Invasive lobular carcinoma on core biopsy
Tumor size on pre-treatment imaging ≤ 2cm	Lymphovascular invasion on core biopsy
Grade 1–2 on pre-treatment core biopsy	Any clinical nodal or metastatic disease
Oestrogen receptor (ER) and Progesterone (PR) positive (> 10%)	Human epidermal growth factor receptor 2 (HER2) positive
Clinically node negative	Prior non-hormonal therapy
Breast primary tumor visible on MR radiation oncology imaging (with or without IV contrast) for treatment localization	Skin or chest wall involvement
	Collagen vascular disease (e.g. lupus, scleroderma)
	Pregnant or lactating
	Absolute contraindications to MRI (e.g. incompatible implants, unable to tolerate duration)

Baseline evaluation included clinical examination, core biopsy, and pre-treatment imaging for diagnosis and radiotherapy planning. The gross tumour volume (GTV) was expanded by 15 mm, limited posteriorly

by the pectoralis muscle and within 5 mm of the skin, to define the clinical target volume (CTV). A uniform 3 mm isotropic margin was then applied to generate the planning target volume (PTV). Patients received a single 21 Gray (Gy) fraction radiotherapy dose delivered on the Elekta Unity 1.5 T MRI-linac with real-time cine MRI monitoring and online adaptive planning. MRI was performed at baseline and five weeks post-treatment, with surgery scheduled one week later. Given the exploratory nature of this trial at our institution, the selected dose and treatment interval for early response assessment were based on prior studies [2,4,5,7] demonstrating clinical effectiveness without significant radiotherapy-related toxicity and with favorable quality-of-life outcomes.

MRI Acquisition Protocol

MRI Acquisition Protocol
Patients underwent pre- and post-treatment imaging on a 1.5 T scanner (Ingenia Ambition, Philips Healthcare, Best, The Netherlands) in the prone position using a dedicated 7-channel breast coil for bilateral coverage. The protocol included a pre-contrast high-spatial and high-temporal resolution axial 3D THRIVE sequence, T1 mapping at flip angles of 5° and 15°, and axial T2-weighted fat-suppressed imaging. DWI was acquired with b-values of 0 and 800 s/mm², and apparent diffusion coefficient (ADC) maps were generated using a mono-exponential fit, with low ADC values appearing dark. DCE- MRI was performed following intravenous gadolinium administration (3 mL/s) with a 15 mL saline flush. High-temporal resolution DCE captured 28 dynamic volumes during the first 2 minutes, followed by five high-spatial resolution series acquired at 60-second intervals over approximately 6 minutes. Both DCE protocols used a T1-weighted fast-field echo (spoiled gradient echo) acquisition, and all sequences employed spectral attenuated inversion recovery (SPAIR) for fat suppression. Detailed acquisition parameters are provided in Supplementary Table 1.

Standard DCE-MRI: Morphological analysis:

Radiologic response was quantitatively assessed by an expert breast radiologist using a picture archiving and communication system (PACS; General Electric Medical Systems, Milwaukee, WI). Lesion size was measured as the maximum axial diameter with two perpendicular orthogonal dimensions. Tumour volume was calculated using the cubic model (D1 × D2 × D3).

Apparent Diffusion Coefficient Analysis:

DWI datasets were transferred to the Intelli-Space Portal (version 12.1; Philips Healthcare) and processed using the diffusion analysis package. Lesions were identified on high-b value images (800 s/mm²) and verified on corresponding ADC maps. Regions of interest (ROIs) were manually contoured to encompass the GTV on all slices containing tumour, with contiguous ROIs drawn across slices. Mean ADC was derived as the average across all ROIs.

Standard DCE-MRI: Intra-tumoral habitat analysis:

Voxel-wise SER mapping was performed to evaluate spatial heterogeneity of contrast kinetics within the tumor. Analyses were conducted in 3D Slicer (version 5.8.1, www.slicer.org) using an inhouse Python-based SER module. To correct for motion between pre- and post-contrast acquisitions, image volumes were co-registered using the Advanced Normalization Tools (ANTs) framework. Tumor regions of interest (ROIs) were manually segmented on the first post-contrast volume and reviewed by a breast radiologist for accuracy.

Percent enhancement (PE) for each voxel was defined as (S1 – S0)/S0, where S0 is the pre-contrast signal intensity and S1 the first post-contrast signal intensity. The SER ratio was defined as (S1 – S0)/(S2 – S0), where S2 is the delayed post-contrast signal intensity. To minimise noise, voxels were required to meet both a 50% PE threshold and a 60% baseline enhancement filter. These thresholds were defined a priori based on criteria established in the American College of Radiology Imaging Network 6657 protocol, which recommends a minimum enhancement threshold of 50% for voxel inclusion, with higher thresholds (up to 100%) permitted depending on study design and signal-to-noise considerations [16,33]. The 50% PE threshold was selected as a conservative lower bound, consistent with prior neoadjuvant breast MRI trials [34–36], to balance sensitivity to treatment-related vascular changes while suppressing background noise

Eligible voxels were then classified into kinetic habitats: washout (SER > 1.3), plateau (SER 0.9–1.3), or persistent (SER < 0.9 but > 0). Non-tumor enhancing structures such as vessels, skin, or implant edges were manually excluded.

Peak PE and peak SER were defined as the highest mean values within a cluster of at least nine contiguous voxels (3 × 3 × 3). Volumetric measures were calculated as washout volume (SER > 1.3), plateau volume (SER 0.9–1.3), and persistent volume (SER 0–0.9), expressed in mm^3.

Ultrafast DCE-MRI analysis:

Ultrafast MRI data were analysed using the perfusion module of Philips Intelli-Space Portal (version 12.1, Philips Healthcare). For each lesion, the GTV was delineated on all slices where the tumour was visible, with contiguous ROIs drawn to fully encompass the GTV. The mean signal intensity across all ROIs was then calculated and used for kinetic analysis. Ultrafast semi-quantitative parameters were then generated, including: Max Signal Enhancement (maximum signal enhancement at the last phase of the ultrafast sequence SI_{max}%), time to peak (TTP, seconds from contrast arrival to SI_{max}%), Wash in Rate (WIR: SI_{max}% ÷ TTP, %/s), Maximum Slope (MS, greatest instantaneous rate of signal change, %/s), and Area Under the Curve (AUC, integrated signal over the enhancement period).

Evaluation histopathology

Core biopsy specimens were evaluated for histologic type, tumor grade (Elston–Ellis modification of the Bloom–Richardson system), immunohistochemical receptor status (ER, PR, and HER2), with positivity defined according to ASCO/CAP guidelines [37,38]. Surgical specimens were sliced at 5-mm intervals, fixed in 10% neutral-buffered formalin, paraffin-embedded, and stained with hematoxylin and eosin. Final pathology was reviewed for the same features as the biopsies, as well as surgical margin status, sentinel lymph node involvement, and the longest dimension of residual tumor [39]. All specimens were examined by a single subspecialized breast pathologist with over 14 years' experience, blinded to MRI findings.

Pathologic response was graded using the Miller–Payne system, a five-point scale based on reduction in tumor cellularity: grade 1, no reduction; grade 2, minor reduction (< 30%); grade 3, 30–90% reduction; grade 4, > 90% reduction (near-complete response); and grade 5, complete absence of malignant cells (pathologic complete response) [40]. Pathologic response was then defined accordingly: with grade 5 defined as pathologic complete response (pCR), grades 3–4 as partial response (pPR), and grades 1–2 as non-response (pNR) [41].

Statistical Analysis

Given the exploratory nature and small sample size, analyses focused on descriptive summaries. MRI parameters were summarized as medians with minimum and maximum ranges.

All analyses were conducted in SPSS (version 30.0.0.0; IBM Corp., Armonk, NY, USA).

Results

Patient Cohort and Baseline Characteristics

Since trial initiation in 2022, 18 patients were enrolled; nine completed both baseline and post-treatment MRI and were included in the final paired analysis. Figure 1 summarises patient disposition and reasons for exclusion. Baseline scans were performed a median of 8 days before treatment, with post-treatment imaging at 34 days (baseline-to-post interval 42 days), and surgery a median of 13 days later.

The median age was 69 years (range, 62–84). Baseline MRI showed tumors 3–14 mm in diameter (median, 10 mm). All were invasive ductal carcinoma of no special type (IDC-NST), with one also demonstrating ductal carcinoma in situ (DCIS). All patients were prescribed neoadjuvant endocrine therapy with an aromatase inhibitor (letrozole or anastrozole) following diagnosis. Eight (89%) completed and continued therapy, one (11%) discontinued due to arthralgia. Baseline and post-treatment clinicopathologic features are summarized in Table 2.

Table 2
shows tumor type, grade, and biomarker results (ER, PR, HER2) recorded at core biopsy and at the final surgical specimen.

Tumor Type	Grade Core	ER Core (%)	PR Core (%)	HER2 Core Status	Grade Final	ER Final (%)	PR Final (%)	HER2 Final Status
Invasive ductal carcinoma (NST)	2	50	10	0	2	30	0	0
Invasive breast carcinoma (NST)	2	100	50	0	1	90	15	0
Invasive ductal carcinoma (NST)	1	95	2	0	1	99	0	0
Invasive breast carcinoma (NST)	2	95	80	0	1	50	0	0
Invasive ductal carcinoma (NST)	2	95	95	0	1	90	90	0
Invasive ductal carcinoma (NST)	2	90	15	0	1	100	0	0
Invasive ductal carcinoma (NST)	2	95	80	0	2	95	0	0
Invasive breast carcinoma (NST) with DCIS	1	90	0	0	1	100	80	0
Invasive ductal carcinoma (NST)	1	90	90	0	1	90	0	0

Pathological response

On final histopathology, no patient achieved pCR. six of 9 patients (67%) demonstrated a pPR, while three (33%) had pNR. Residual tumor size ranged from 4–24 mm (median, 13 mm).

MRI Analysis

Changes across all patients before and after therapy

Post-treatment imaging demonstrated a redistribution of SER patterns toward lower enhancement categories. Both intermediate-enhancing voxels (SER 0.90–1.30) and late-phase washout (SER 1.30–3.00) were reduced from 193mm^3 to 82mm^3 & 12 mm³ to 3 mm³, respectively, while peak SER decreased from 0.98 to 0.83, reflecting a shift toward lower enhancement. ADC also rose from 0.99 × 10^{-3} to 1.18 × 10^{-3} mm²/s, and tumor volume declined from 1144 mm³ to 700 mm³. Longest diameter showed minimal change. Among ultrafast parameters, SI_{max} decreased from 52% to 43% post therapy, while other parameters (AUC, MS, WIR) remained stable. Semiquantitative and diffusion parameter values are shown in Table 3.

Table 3
Changes across all patients before and after NRT. Values are presented as median [range].

MRI Metric	Before NRT (n = 9)	After NRT (n = 9)
Morphological		
Longest Diameter (mm)	13 [5–19]	10 [4–19]
Tumor Volume (mm^3)	1144 [45–3705]	700 [36–3192]
Diffusion		
ADC ($x10^{-3}$ mm^2/s)	0.99 [0.70–1.25]	1.18 [0.83–1.65]
Conventional DCE		
SER 0-0.9 (mm^3)	236 [51–694]	220 [98–736]
SER 0.9–1.3 (mm^3)	193 [16–538]	82 [33–252]
SER 1.3-3.0 (mm^3)	12 [1–53]	3 [0–32]
pSER	0.98 [0.58–1.27]	0.83 [0.46–1.18]
pPE (%)	111.8 [39.1–195.7]	88.1 [51.9–179.9]
Ultrafast DCE		
SI_{max}(%)	51.6 [30.4–102.6]	42.9 [31.2–101.7]
TTP (sec)	101.5 [61.1–112.3]	108.7 [64.7–108.7]
MS %/s	7.4 [2.6–14.4]	6.7 [3.0–13.5]
AUC	23,437 [10,986–69,852]	22,631 [14,633–44,590]
WIR (%/s)	25.8 [13.5–59.4]	25.6 [15.0–53.5]

Grouped by partial pathologic response

Analyses stratified by partial pathological response are presented in Table 4. Among the MRI parameters analysed, ADC showed a greater percentage increase in partial responders compared with non-responders (44.5% vs 11.1%; Fig. 2). In contrast, percentage changes in longest diameter and tumour volume were numerically similar between groups.

Table 4
Values are median [range].

MRI Metric	Partial Responders (n = 6) Pre	Post	Median % Change†	Non-Responders (n = 3) Pre	Post	Median % Change†
Morphological						
Longest diameter (mm)	13 [8–19]	11.5 [8–19]	−11.5	8 [5–13]	8 [4–13]	0
Tumour volume (mm³)	1292 [200–3705]	994 [200–3192]	−18.1	448 [45–1716]	336 [36–1430]	−20.0
Diffusion						
ADC (×10⁻³ mm²/s)	1.07 [0.70–1.25]	1.40 [1.07–1.65]	44.5	0.92 [0.83–0.99]	1.10 [0.83–1.10]	11.1
Conventional DCE						
SER 0–0.9 (mm³)	365 [87–694]	419 [147–736]	35.8	96 [51–237]	132 [98–355]	75
SER 0.9–1.3 (mm³)	193 [88–538]	82 [33–230]	−61.2	91 [16–472]	82 [48–252]	−46.6
SER 1.3–3.0 (mm³)	11 [1–53]	5 [0–32]	−99.1	38 [4–47]	30 [8–30]	−59.6
pSER	0.95 [0.64–1.14]	0.73 [0.46–0.95]	−23.9	1.13 [0.58–1.27]	0.96 [0.79–1.18]	−7.1
pPE (%)	112.3 [54.4–153.8]	83.6 [51.9–120.7]	−14.1	90.8 [39.1–195.7]	88.0 [55.0–179.9]	−3.1
Ultrafast DCE						
SImax (%)	74.3 [30.4–102.6]	40.2 [31.2–101.7]	−29.9	46.7 [34.0–47.6]	53.4 [44.0–71.1]	14.4
TTP (s)	101.5 [64.7–112.3]	108.7 [68.3–108.7]	3.1	97.9 [61.1–101.5]	101.5 [64.7–108.7]	5.9
MS (%/s)	9.8 [3.5–14.4]	7.1 [3.0–13.0]	−13.3	5.0 [2.6–13.4]	5.3 [4.1–13.5]	6

†Percentage change calculated per participant as ((post − pre) / pre) × 100 and summarised as the median percentage change within each response group.

MRI Metric	Partial Responders (n = 6) Pre	Post	Median % Change†	Non-Responders (n = 3) Pre	Post	Median % Change†
Morphological						
AUC	23836 [15657–69852]	17471 [14633–44590]	−11.8	23437 [10986–35829]	24979 [22631–32776]	6.6
WIR (%/s)	32.1 [13.5–59.4]	22.3 [15.0–53.5]	−2.2	25.8 [14.2–58.2]	26.5 [24.0–49.9]	−7.0

†Percentage change calculated per participant as ((post − pre) / pre) × 100 and summarised as the median percentage change within each response group.

For DCE-MRI–derived measures, partial responders exhibited larger reductions in peak SER and peak PE. SER voxel analysis demonstrated differences in enhancement distribution: non-responders showed a greater proportional increase in low-enhancing voxels post-treatment (75.0% vs 35.8%), whereas partial responders demonstrated a larger reduction in washout voxels (99.1% vs 59.6%).

Across ultrafast DCE parameters, small directional differences were observed between partial responders and non-responders; however, substantial overlap in individual values remained between groups (Fig. 3).

Discussion

Early detection of treatment response is clinically valuable, enabling personalised adaptation of therapy, minimising unnecessary toxicity, and avoiding prolonged ineffective treatment in non-responders. Achieving this, however, requires imaging biomarkers that are both accurate and reproducible. This study aimed to evaluate the feasibility of mp-MRI for detecting early biological changes following SF-NRT in patients with early-stage breast cancer, approximately five weeks post-treatment. In this prospective cohort, functional MRI revealed biologically plausible directional changes consistent with treatment response. Increased ADC values were observed in partial responders, accompanied by reductions in intravoxel washout fraction, peak SER, and peak PE. In contrast, morphological parameters showed minimal or inconsistent change. While the limited sample size precludes definitive conclusions, these exploratory findings provide preliminary evidence that functional MRI may capture early treatment-induced microstructural and vascular adaptations that precede measurable morphologic regression.

Treatment response has traditionally been evaluated using morphologic criteria such as the longest tumour diameter or overall volume, valued for their simplicity and reproducibility [10,12,16,42–45]. Several NAC studies have shown that volumetric analysis provides superior early predictive value compared with unidimensional measurements [13,16,45–47]. In our study, tumour volume declined more than longest diameter following treatment; however, when stratified by pathological response, neither metric showed

clear separation between partial responders and non-responders. High inter-patient variability likely contributed to this finding. For example, one partial responder showed a paradoxical 12% increase in volume post treatment, possibly reflecting inflammatory changes rather than true disease progression. Morphologic response data after SF-NRT are scarce. One study [48] using a hypo fractionated regimen reported superior predictive accuracy for volumetric versus linear metrics, though the discrepancy with our results may reflect radiobiological differences between single- and multi-fraction regimens, the small sample size, or the early imaging timepoint. Given these limitations, our morphological findings should be interpreted cautiously and require validation in larger cohorts.

Intra tumoral habitat analysis provided complementary physiological insights. In our study, intravoxel SER mapping revealed a redistribution of enhancement patterns characterised by reductions in intermediate-enhancing and washout voxels and a decline in peak SER and peak PE. This global shift toward lower enhancement likely represents a loss of highly vascularised tumour components and the onset of vascular normalisation [15,49–51], changes most evident in partial responders. These findings align with prior SF-NRT data. Vasmel et al. reported an 89% reduction in washout voxel volume among responders compared with 17% in non-responders at six months [31]. In our cohort, the respective reductions were 99.1% and 59.6%, representing a smaller separation between groups, likely reflecting both the earlier imaging timepoint and cohort size. Nonetheless, the consistency of directional change across studies suggests that vascular alterations may be captured as early as five weeks post treatment, potentially preceding measurable sized based shrinkage. In contrast to semi-quantitative SER-based habitat analysis, ultrafast DCE parameters did not demonstrate a similar discriminatory pattern. Ultrafast DCE-MRI parameters, which capture rapid contrast vascular kinetics during initial uptake [19,20,22,52,53], showed large inter-patient variability with no apparent differences between partial responders and non-responders. Similar inconsistencies have been noted in the NAC literature [19,53,54]. For example, Kim et al. [53] found that ultrafast parameters did not predict pCR across breast cancer subtypes, whereas Ramtohul et al. [19] observed higher wash-in rates in pCR responders. These conflicting results likely arise from differences in sample size, tumour subtype, acquisition protocol, and kinetic modelling approach. In our cohort imaged at 5 weeks post SF-NRT, ultrafast parameters did not demonstrate utility for early response assessment. Whether this reflects the early imaging timepoint, the low-grade HR+ tumour biology, technical limitations, or true lack of predictive value remains unclear. Larger studies with standardized acquisition protocols and subtype stratification are needed before ultrafast MRI can be recommended for routine response assessment following SF-NRT.

In our study, ADC, a measure of water molecule diffusivity [27], showed the largest treatment-associated increase following SF-NRT. Partial responders demonstrated a median percentage ADC increase of 44.5%, compared with 11.1% in non-responders. Although this difference did not reach statistical significance due to the small sample size, the directional trend is consistent with microstructural alterations, including reduced tumour cellularity, radiation-induced lysis, membrane degradation, and expansion of the extracellular space [9,55,56]. These observations are directionally consistent with prior SF-NRT data. Vasmel et al. [31] similarly reported statistically significant ADC increases at six months

following SF-NRT (48.3% vs 23.4% in responders vs non-responders), with trends emerging from four months onwards (41.4% vs 28.6%). While ADC changes have been observed as early as one week post-treatment [29–31] these early shifts are often attributed to acute inflammatory effects rather than true tumour regression. As prior data suggest that treatment-induced changes become more reliably distinguishable from inflammation by four to six months, our five-week timepoint may represent an early–intermediate phase of response evolution. The directional consistency between our findings and those reported at later intervals raises the possibility that genuine microstructural changes may already be emerging; however, confirmation through serial imaging and histopathological correlation is required to definitively characterise the biological basis of these early signal alterations.

Finally, none of the patients in our study achieved pCR, likely reflecting the short interval between treatment and surgery. Prior SF-NRT studies demonstrate increasing pCR rates with longer time-to-surgery intervals. Vasmel et al. [31] reported pCR rates of 33% at 6 months and 48% at 8 months following SF-NRT, while Rahimi et al. [57] showed that in patients undergoing delayed surgery (> 9 months), overall pCR reached 72%, with longer time to surgery — rather than higher radiation dose — significantly associated with pCR (OR 1.02). Although multi-fraction regimens have reported lower early pCR rates (23% in the PAPBI trial at 6 weeks [58] and 15% at 3 weeks in Nichols et al. using ten fractions of 3.85 Gy [59]) differences in fractionation schedules limit direct comparison with our single-fraction approach. Our surgical timepoint at 6 weeks post-SF-NRT likely preceded the interval at which complete pathological regression becomes evident. Accordingly, the functional MRI changes observed in partial responders may represent early biological alterations that precede eventual pathological regression. Imaging at this early interval may nevertheless offer a pragmatic clinical opportunity: identification of early responders could support extended observation or delayed surgery strategies, whereas early recognition of non-responders may enable timely treatment escalation. In this way, therapeutic pathways could be individualised according to biological response rather than fixed temporal criteria. Prospective validation in larger cohorts is required before such strategies can be considered for clinical implementation.

Limitations and Future research:

Although our exploratory findings suggest that several MRI metrics may serve as promising imaging biomarkers for response assessment, several limitations should be acknowledged. First, the study's small sample size is a key constraint. The RICE trial initially aimed to recruit 30 participants but was terminated early due to an unexpectedly high rate of postoperative infections. Therefore, our findings should be interpreted with caution. Nonetheless, even with this limited sample size, we observed biologically plausible radiological changes between partial responders and non-responders. Second, our cohort consisted exclusively of postmenopausal women with low-grade, HR+ tumours, a cohort "potentially suitable" for SF-NRT [60–62]. While this design choice intentionally reduced biological heterogeneity to ensure safety and feasibility, it limits generalisability to more aggressive tumour subtypes. Third, full quantitative pharmacokinetic perfusion modelling was not performed in this study, as imaging parameters were not optimised for such analysis. Nevertheless, given that prior studies in

the NAC setting have demonstrated strong correlations between semi-quantitative time–signal intensity parameters and fully quantitative perfusion measures, we argue that our use of semi-quantitative analysis represents a more practical and clinically feasible approach for routine implementation [14,16,29,31,63].

Future research should expand upon our preliminary findings in several key ways. First, validation in larger, prospective cohorts is essential to confirm the reproducibility of the functional imaging biomarkers identified as potentially useful for early response assessment. Second, the optimal imaging timepoint for distinguishing genuine treatment response from residual inflammatory effects remains undefined. Although previous studies [29,31] have examined functional MRI at very early post-treatment intervals, few have correlated these findings with corresponding histopathological changes. We therefore recommend that future investigations incorporate serial mp-MRI during the early post-SF-NRT period with paired histopathological sampling where feasible, to characterize the temporal evolution of imaging biomarkers and establish the earliest interval at which functional parameters reliably reflect true treatment response. Our findings at five weeks suggest this may be an important transitional window, but prospective validation with pathological correlation is essential.

Conclusion

This exploratory analysis from the RICE trial provides preliminary evidence that functional MRI metrics, including ADC and intravoxel enhancement redistribution, exhibit biologically plausible directional changes at five weeks following SF-NRT, with observable differences between response groups. While morphological parameters demonstrated minimal change at this early timepoint, functional measures showed patterns consistent with microstructural and vascular alterations in partial responders, suggesting that physiological imaging biomarkers may provide complementary value to conventional size-based criteria for early response assessment. However, the small sample size, absence of pCR, and descriptive nature of these findings preclude definitive conclusions. Validation in larger, independent cohorts with standardized imaging protocols and longer follow-up is required to determine the reproducibility, optimal timing, and clinical utility of functional MRI for response prediction after SF-NRT. If confirmed, early functional imaging could support more individualized treatment strategies, such as delayed surgery in partial responders or timely treatment escalation in non-responders, with the goal of optimizing outcomes in patients undergoing neoadjuvant radiotherapy.

Abbreviations

- **ADC**
Apparent Diffusion Coefficient
- **AUC**
Area Under the Curve
- **CTV**
Clinical Target Volume

• **DCIS**
Ductal Carcinoma In Situ
• **DCE**
MRI–Dynamic Contrast–Enhanced Magnetic Resonance Imaging
• **DWI**
Diffusion–Weighted Imaging
• **ER+**
Estrogen Receptor Positive
• **GTV**
Gross Tumour Volume
• **Gy**
Gray
• **HER2**
Human Epidermal Growth Factor Receptor 2
• **IDC**
NST–Invasive Ductal Carcinoma of No Special Type
• **mp**
MRI–Multiparametric Magnetic Resonance Imaging
• **MRI**
Magnetic Resonance Imaging
• **MS**
Maximum Slope
• **PE**
Percent Enhancement
• **pCR**
Pathologic Complete Response
• **pNR**
Pathologic Non–Response
• **pPR**
Partial Pathologic Response
• **PR+**
Progesterone Receptor Positive
• **PTV**
Planning Target Volume
• **RICE**
Magnetic Resonance Imaging–guided Single–Fraction Preoperative Radiotherapy for Early–Stage Breast Cancer (Feasibility Study)
• **ROI**
Region of Interest
• **S0**

Pre–contrast Signal Intensity
• **S1**
First Post–contrast Signal Intensity
• **S2**
Delayed Post–contrast Signal Intensity
• **SER**
Signal Enhancement Ratio
• **SF**
NRT–Single–Fraction Neoadjuvant Radiotherapy
• **SImax**
Maximum Signal Intensity
• **TTP**
Time to Peak
• **WIR**
Wash–in Rate

Declarations

Acknowledgements-None

Ethics Approval Statement- This study and associated patient information sheets have been approved by the Austin Health Human Research and Ethics Committee (HREC). HREC Reference: HREC: CPMP/ICH-135/95.

Informed Consent Statement- Written informed consent was obtained from all participants involved in the study prior to enrolment. The study was conducted in accordance with the Declaration of Helsinki and was approved by the institutional Human Research Ethics Committee.

Declaration of Conflicting Interests- The authors declared no potential conflicts of interest with respect to the research, authorship, and/or publication of this article.

Data Availability- The datasets analyzed during the current study are available from the corresponding author on reasonable request.

Funding- This study is funded by the National Breast Cancer Foundation (NBCF) (grant number: IIRS-20–097) who has no role in collection, analysis, and interpretation of data or in writing the manuscript.

Authors contribution-

Ayyaz Qadir prepared and wrote the initial draft and designed the manuscript methodology.

All authors contributed to the review and editing of the final manuscript.

All authors have approved the final version of the manuscript. All persons designated as authors qualify for authorship and all those that qualify have been listed as authors.

References

1. Meattini I, Francolini G, Di Cataldo V, et al. Preoperative robotic radiosurgery for early breast cancer: Results of the phase II ROCK trial (NCT03520894). *Clin Transl Radiat Oncol*. Nov 2022;37:94-100. doi:10.1016/j.ctro.2022.09.004
2. Tiberi D, Vavassis P, Nguyen D, et al. Tumour response 3 months after neoadjuvant single-fraction radiotherapy for low-risk breast cancer. *Curr Oncol*. Jun 2020;27(3):155-158. doi:10.3747/co.27.6059
3. Lavigne D, Hijal T, Vavassis P, et al. Single preoperative radiation therapy with delayed surgery for low-risk breast cancer: Oncologic outcome, toxicity and cosmesis of the SPORT-DS phase I trial. *Radiother Oncol*. Nov 2024;200:110515. doi:10.1016/j.radonc.2024.110515
4. Guidolin K, Yaremko B, Lynn K, et al. Stereotactic image-guided neoadjuvant ablative single-dose radiation, then lumpectomy, for early breast cancer: the SIGNAL prospective single-arm trial of single-dose radiation therapy. *Curr Oncol*. Jun 2019;26(3):e334-e340. doi:10.3747/co.26.4479
5. Vasmel JE, Charaghvandi RK, Houweling AC, et al. Tumor Response After Neoadjuvant Magnetic Resonance Guided Single Ablative Dose Partial Breast Irradiation. *Int J Radiat Oncol Biol Phys*. Mar 15 2020;106(4):821-829. doi:10.1016/j.ijrobp.2019.11.406
6. Rahimi A, Simmons A, Kim DN, et al. Preliminary Results of Multi-Institutional Phase 1 Dose Escalation Trial Using Single-Fraction Stereotactic Partial Breast Irradiation for Early Stage Breast Cancer. *Int J Radiat Oncol Biol Phys*. Mar 1 2022;112(3):663-670. doi:10.1016/j.ijrobp.2021.10.010
7. Horton JK, Blitzblau RC, Yoo S, et al. Preoperative Single-Fraction Partial Breast Radiation Therapy: A Novel Phase 1, Dose-Escalation Protocol With Radiation Response Biomarkers. *Int J Radiat Oncol Biol Phys*. Jul 15 2015;92(4):846-55. doi:10.1016/j.ijrobp.2015.03.007
8. Janssen LM, den Dekker BM, Gilhuijs KGA, van Diest PJ, van der Wall E, Elias SG. MRI to assess response after neoadjuvant chemotherapy in breast cancer subtypes: a systematic review and meta-analysis. *NPJ Breast Cancer*. Sep 19 2022;8(1):107. doi:10.1038/s41523-022-00475-1
9. Qadir A, Singh N, Moe AAK, et al. Potential of MRI in Assessing Treatment Response After Neoadjuvant Radiation Therapy Treatment in Breast Cancer Patients: A Scoping Review. *Clinical Breast Cancer*. 2025;25(1):e1-e9.e2. doi:10.1016/j.clbc.2024.05.010
10. Liang X, Chen X, Yang Z, et al. Early prediction of pathological complete response to neoadjuvant chemotherapy combining DCE-MRI and apparent diffusion coefficient values in breast Cancer. *BMC Cancer*. Dec 2 2022;22(1):1250. doi:10.1186/s12885-022-10315-x
11. Pereira NP, Curi C, Osório CABT, et al. Diffusion-Weighted Magnetic Resonance Imaging of Patients with Breast Cancer Following Neoadjuvant Chemotherapy Provides Early Prediction of Pathological Response – A Prospective Study. *Scientific Reports*. 2019/11/08 2019;9(1):16372. doi:10.1038/s41598-019-52785-3

12. Moloney B, Li X, Hirano M, et al. Initial experience in implementing quantitative DCE-MRI to predict breast cancer therapy response in a multi-center and multi-vendor platform setting. *Front Oncol*. 2024;14:1395502. doi:10.3389/fonc.2024.1395502
13. Partridge SC, Gibbs JE, Lu Y, et al. MRI measurements of breast tumor volume predict response to neoadjuvant chemotherapy and recurrence-free survival. *AJR Am J Roentgenol*. Jun 2005;184(6):1774-81. doi:10.2214/ajr.184.6.01841774
14. Li KL, Henry RG, Wilmes LJ, et al. Kinetic assessment of breast tumors using high spatial resolution signal enhancement ratio (SER) imaging. *Magn Reson Med*. Sep 2007;58(3):572-81. doi:10.1002/mrm.21361
15. Arasu VA, Chen RC, Newitt DN, et al. Can signal enhancement ratio (SER) reduce the number of recommended biopsies without affecting cancer yield in occult MRI-detected lesions? *Acad Radiol*. Jun 2011;18(6):716-21. doi:10.1016/j.acra.2011.02.008
16. Hylton NM, Blume JD, Bernreuter WK, et al. Locally advanced breast cancer: MR imaging for prediction of response to neoadjuvant chemotherapy--results from ACRIN 6657/I-SPY TRIAL. *Radiology*. Jun 2012;263(3):663-72. doi:10.1148/radiol.12110748
17. Partridge SC, Zhang Z, Newitt DC, et al. Diffusion-weighted MRI Findings Predict Pathologic Response in Neoadjuvant Treatment of Breast Cancer: The ACRIN 6698 Multicenter Trial. *Radiology*. Dec 2018;289(3):618-627. doi:10.1148/radiol.2018180273
18. Jones EF, Hathi DK, Freimanis R, et al. Current Landscape of Breast Cancer Imaging and Potential Quantitative Imaging Markers of Response in ER-Positive Breast Cancers Treated with Neoadjuvant Therapy. *Cancers*. 2020;12(6):1511.
19. Ramtohul T, Tescher C, Vaflard P, et al. Prospective Evaluation of Ultrafast Breast MRI for Predicting Pathologic Response after Neoadjuvant Therapies. *Radiology*. Dec 2022;305(3):565-574. doi:10.1148/radiol.220389
20. Ohashi A, Kataoka M, Kanao S, et al. Diagnostic performance of maximum slope: A kinetic parameter obtained from ultrafast dynamic contrast-enhanced magnetic resonance imaging of the breast using k-space weighted image contrast (KWIC). *Eur J Radiol*. Sep 2019;118:285-292. doi:10.1016/j.ejrad.2019.06.012
21. Ohashi A, Kataoka M, Iima M, et al. Comparison of Ultrafast Dynamic Contrast-Enhanced (DCE) MRI with Conventional DCE MRI in the Morphological Assessment of Malignant Breast Lesions. *Diagnostics (Basel)*. Mar 15 2023;13(6)doi:10.3390/diagnostics13061105
22. Kataoka M, Honda M, Sagawa H, et al. Ultrafast Dynamic Contrast-Enhanced MRI of the Breast: From Theory to Practice. *Journal of Magnetic Resonance Imaging*. 2024;60(2):401-416. doi:https://doi.org/10.1002/jmri.29082
23. Tudorica A, Oh KY, Chui SY, et al. Early prediction and evaluation of breast cancer response to neoadjuvant chemotherapy using quantitative DCE-MRI. *Translational oncology*. 2016;9(1):8-17.
24. Li X, Arlinghaus LR, Ayers GD, et al. DCE-MRI analysis methods for predicting the response of breast cancer to neoadjuvant chemotherapy: Pilot study findings. *Magnetic resonance in medicine*.

2014;71(4):1592-1602.

25. Sharma A, Sharma S, Sood S, Seam RK, Sharma M, Fotedar V. DCE-MRI and parametric imaging in monitoring response to neoadjuvant chemotherapy in breast carcinoma: a preliminary report. *Polish Journal of Radiology*. 2018;83:220-228.
26. Ah-See M-LW, Makris A, Taylor NJ, et al. Early changes in functional dynamic magnetic resonance imaging predict for pathologic response to neoadjuvant chemotherapy in primary breast cancer. *Clinical Cancer Research*. 2008;14(20):6580-6589.
27. Chu W, Jin W, Liu D, et al. Diffusion-weighted imaging in identifying breast cancer pathological response to neoadjuvant chemotherapy: A meta-analysis. *Oncotarget*. Jan 23 2018;9(6):7088-7100. doi:10.18632/oncotarget.23195
28. Cheng Q, Huang J, Liang J, et al. The Diagnostic Performance of DCE-MRI in Evaluating the Pathological Response to Neoadjuvant Chemotherapy in Breast Cancer: A Meta-Analysis. *Front Oncol*. 2020;10:93. doi:10.3389/fonc.2020.00093
29. Wang C, Horton JK, Yin FF, Chang Z. Assessment of Treatment Response With Diffusion-Weighted MRI and Dynamic Contrast-Enhanced MRI in Patients With Early-Stage Breast Cancer Treated With Single-Dose Preoperative Radiotherapy: Initial Results. *Technol Cancer Res Treat*. Oct 2016;15(5):651-60. doi:10.1177/1533034615593191
30. Mouawad M, Biernaski H, Brackstone M, et al. DCE-MRI assessment of response to neoadjuvant SABR in early stage breast cancer: Comparisons of single versus three fraction schemes and two different imaging time delays post-SABR. *Clin Transl Radiat Oncol*. Mar 2020;21:25-31. doi:10.1016/j.ctro.2019.12.004
31. Vasmel JE, Groot Koerkamp ML, Mandija S, et al. Dynamic Contrast-enhanced and Diffusion-weighted Magnetic Resonance Imaging for Response Evaluation After Single-Dose Ablative Neoadjuvant Partial Breast Irradiation. *Adv Radiat Oncol*. Mar-Apr 2022;7(2):100854. doi:10.1016/j.adro.2021.100854
32. Qadir A, Singh N, Dean J, et al. Magnetic resonance imaging-guided single-fraction preoperative radiotherapy for early-stage breast cancer (the RICE trial): feasibility study. *Pilot and Feasibility Studies*. 2024/11/07 2024;10(1):133. doi:10.1186/s40814-024-01557-6
33. Lo W-C, Li W, Jones EF, et al. Effect of Imaging Parameter Thresholds on MRI Prediction of Neoadjuvant Chemotherapy Response in Breast Cancer Subtypes. *PLOS ONE*. 2016;11(2):e0142047. doi:10.1371/journal.pone.0142047
34. Henderson SA, Muhammad Gowdh N, Purdie CA, et al. Breast cancer: influence of tumour volume estimation method at MRI on prediction of pathological response to neoadjuvant chemotherapy. *Br J Radiol*. Jul 2018;91(1087):20180123. doi:10.1259/bjr.20180123
35. Musall BC, Abdelhafez AH, Adrada BE, et al. Functional Tumor Volume by Fast Dynamic Contrast-Enhanced MRI for Predicting Neoadjuvant Systemic Therapy Response in Triple-Negative Breast Cancer. *J Magn Reson Imaging*. Jul 2021;54(1):251-260. doi:10.1002/jmri.27557

36. Seo M, Cho N, Bae MS, et al. Features of Undiagnosed Breast Cancers at Screening Breast MR Imaging and Potential Utility of Computer-Aided Evaluation. *Korean J Radiol*. Jan-Feb 2016;17(1):59-68. doi:10.3348/kjr.2016.17.1.59
37. Hammond M, Hayes D, Dowsett M, et al. Pathologists' guideline recommendations for immunohistochemical testing of estrogen and progesterone receptors in breast cancer. *Breast Care*. 2010;5(3):185-7.
38. Singh K, Tantravahi U, Lomme MM, Pasquariello T, Steinhoff M, Sung CJ. Updated 2013 College of American Pathologists/American Society of Clinical Oncology (CAP/ASCO) guideline recommendations for human epidermal growth factor receptor 2 (HER2) fluorescent in situ hybridization (FISH) testing increase HER2 positive and HER2 equivocal breast cancer cases; retrospective study of HER2 FISH results of 836 invasive breast cancers. *Breast cancer research and treatment*. 2016;157(3):405-411.
39. Provenzano E, Bossuyt V, Viale G, et al. Standardization of pathologic evaluation and reporting of postneoadjuvant specimens in clinical trials of breast cancer: recommendations from an international working group. *Modern Pathology*. 2015;28(9):1185-1201.
40. Ogston KN, Miller ID, Payne S, et al. A new histological grading system to assess response of breast cancers to primary chemotherapy: prognostic significance and survival. *Breast*. Oct 2003;12(5):320-7. doi:10.1016/s0960-9776(03)00106-1
41. Choi WJ, Kim WK, Shin HJ, Cha JH, Chae EY, Kim HH. Evaluation of the Tumor Response After Neoadjuvant Chemotherapy in Breast Cancer Patients: Correlation Between Dynamic Contrast-enhanced Magnetic Resonance Imaging and Pathologic Tumor Cellularity. *Clin Breast Cancer*. Feb 2018;18(1):e115-e121. doi:10.1016/j.clbc.2017.08.003
42. Kitajima K, Miyoshi Y, Yamano T, Odawara S, Higuchi T, Yamakado K. Assessment of tumor response to neoadjuvant chemotherapy in patients with breast cancer using MRI and FDG-PET/CT-RECIST 1.1 vs. PERCIST 1.0. *Nagoya J Med Sci*. May 2018;80(2):183-197. doi:10.18999/nagjms.80.2.183
43. Loo CE, Teertstra HJ, Rodenhuis S, et al. Dynamic contrast-enhanced MRI for prediction of breast cancer response to neoadjuvant chemotherapy: initial results. *American Journal of Roentgenology*. 2008;191(5):1331-1338.
44. Martincich L, Montemurro F, De Rosa G, et al. Monitoring response to primary chemotherapy in breast cancer using dynamic contrast-enhanced magnetic resonance imaging. *Breast cancer research and treatment*. 2004;83(1):67-76.
45. Reig B, Heacock L, Lewin A, Cho N, Moy L. Role of MRI to Assess Response to Neoadjuvant Therapy for Breast Cancer. *Journal of Magnetic Resonance Imaging*. 2020;52(6)doi:https://doi.org/10.1002/jmri.27145
46. Lee CS, Moy L. Ultrafast Breast MRI to Predict Pathologic Response after Neoadjuvant Therapy. *Radiology*. 2022/12/01 2022;305(3):575-577. doi:10.1148/radiol.221511
47. Kovacevic L, Petrovecki M, Korsa L, Marusic Z, Dumic-Cule I, Prutki M. Early Assessment of Neoadjuvant Chemotherapy Response Using Multiparametric Magnetic Resonance Imaging in

Luminal B-like Subtype of Breast Cancer Patients: A Single-Center Prospective Study. *Diagnostics*. 2023;13(4). doi:10.3390/diagnostics13040694

48. Weinfurtner RJ, Raghunand N, Stringfield O, et al. MRI Response to Pre-operative Stereotactic Ablative Body Radiotherapy (SABR) in Early Stage ER/PR+ HER2- Breast Cancer correlates with Surgical Pathology Tumor Bed Cellularity. *Clin Breast Cancer*. Feb 2022;22(2):e214-e223. doi:10.1016/j.clbc.2021.06.016
49. Weinfurtner RJ, Abdalah M, Stringfield O, et al. Quantitative Changes in Intratumoral Habitats on MRI Correlate With Pathologic Response in Early-stage ER/PR+ HER2- Breast Cancer Treated With Preoperative Stereotactic Ablative Body Radiotherapy. *J Breast Imaging*. May-Jun 2022;4(3):273-284. doi:10.1093/jbi/wbac013
50. Goedegebuure RS, De Klerk LK, Bass AJ, Derks S, Thijssen VL. Combining radiotherapy with anti-angiogenic therapy and immunotherapy; a therapeutic triad for cancer? *Frontiers in immunology*. 2019;9:3107.
51. Xiao J, Rahbar H, Hippe DS, et al. Dynamic contrast-enhanced breast MRI features correlate with invasive breast cancer angiogenesis. *npj Breast Cancer*. 2021/04/16 2021;7(1):42. doi:10.1038/s41523-021-00247-3
52. Mus RD, Borelli C, Bult P, et al. Time to enhancement derived from ultrafast breast MRI as a novel parameter to discriminate benign from malignant breast lesions. *Eur J Radiol*. Apr 2017;89:90-96. doi:10.1016/j.ejrad.2017.01.020
53. Kim JH, Park VY, Shin HJ, Kim MJ, Yoon JH. Ultrafast dynamic contrast-enhanced breast MRI: Association with pathologic complete response in neoadjuvant treatment of breast cancer. *European Radiology*. 2022;32(7):4823-4833.
54. Choi SE, Park AY, Kim GI, Jung HK, Ko KH, Kim Y. The kinetic parameters of dynamic contrast-enhanced MRI with ultrafast imaging in breast cancer patients receiving neoadjuvant chemotherapy: Prediction of pathologic complete response and correlation with histologic microvessel density. *Medicine (Baltimore)*. Jan 31 2025;104(5):e40239. doi:10.1097/md.0000000000040239
55. Patterson DM, Padhani AR, Collins DJ. Technology Insight: water diffusion MRI—a potential new biomarker of response to cancer therapy. *Nature Clinical Practice Oncology*. 2008/04/01 2008;5(4):220-233. doi:10.1038/ncponc1073
56. Hottat N, Jani J, Badr D, et al. Diffusion-Weighted MRI in the Evaluation of Early-Stage Breast Cancer Treated with a Short Preoperative Radiotherapy: Preliminary Results. *J Belg Soc Radiol*. 2023;107(1):8. doi:10.5334/jbsr.2815
57. Rahimi A, Leitch M, Dogan B, et al. Ablative Preoperative Single-Fraction Radiation Dose Escalation Among Patients With Breast Cancer: A Phase 1 Nonrandomized Clinical Trial. *JAMA Netw Open*. Nov 3 2025;8(11):e2543689. doi:10.1001/jamanetworkopen.2025.43689
58. Bosma SCJ, van der Leij F, Elkhuizen PHM, et al. Evaluation of Early Response to Preoperative Accelerated Partial Breast Irradiation (PAPBI) by Histopathology, Magnetic Resonance Imaging, and

18F-fluorodexoyglucose Positron Emission Tomography/Computed Tomography (FDG PET/CT). *Int J Radiat Oncol Biol Phys*. Jul 15 2021;110(4):1151-1158. doi:10.1016/j.ijrobp.2021.02.033

59. Nichols E, Kesmodel SB, Bellavance E, et al. Preoperative Accelerated Partial Breast Irradiation for Early-Stage Breast Cancer: Preliminary Results of a Prospective, Phase 2 Trial. *Int J Radiat Oncol Biol Phys*. Mar 15 2017;97(4):747-753. doi:10.1016/j.ijrobp.2016.11.030
60. Shaitelman SF, Anderson BM, Arthur DW, et al. Partial Breast Irradiation for Patients With Early-Stage Invasive Breast Cancer or Ductal Carcinoma In Situ: An ASTRO Clinical Practice Guideline. *Practical Radiation Oncology*. 2024;14(2):112-132. doi:10.1016/j.prro.2023.11.001
61. Civil YA, Jonker LW, Groot Koerkamp MPM, et al. Preoperative Partial Breast Irradiation in Patients with Low-Risk Breast Cancer: A Systematic Review of Literature. *Ann Surg Oncol*. Jun 2023;30(6):3263-3279. doi:10.1245/s10434-023-13233-9
62. Qadir A, Singh N, Chui A, Chao M, Uribe S, Foroudi F. Partial Breast Irradiation for Early-Stage Breast Cancer: Advances, Challenges, and Future Directions-A Narrative Review. *Tomography*. May 22 2025;11(6)doi:10.3390/tomography11060059
63. O'Flynn EA, DeSouza NM. Functional magnetic resonance: biomarkers of response in breast cancer. *Breast Cancer Research*. 2011;13(1):204.

Figures

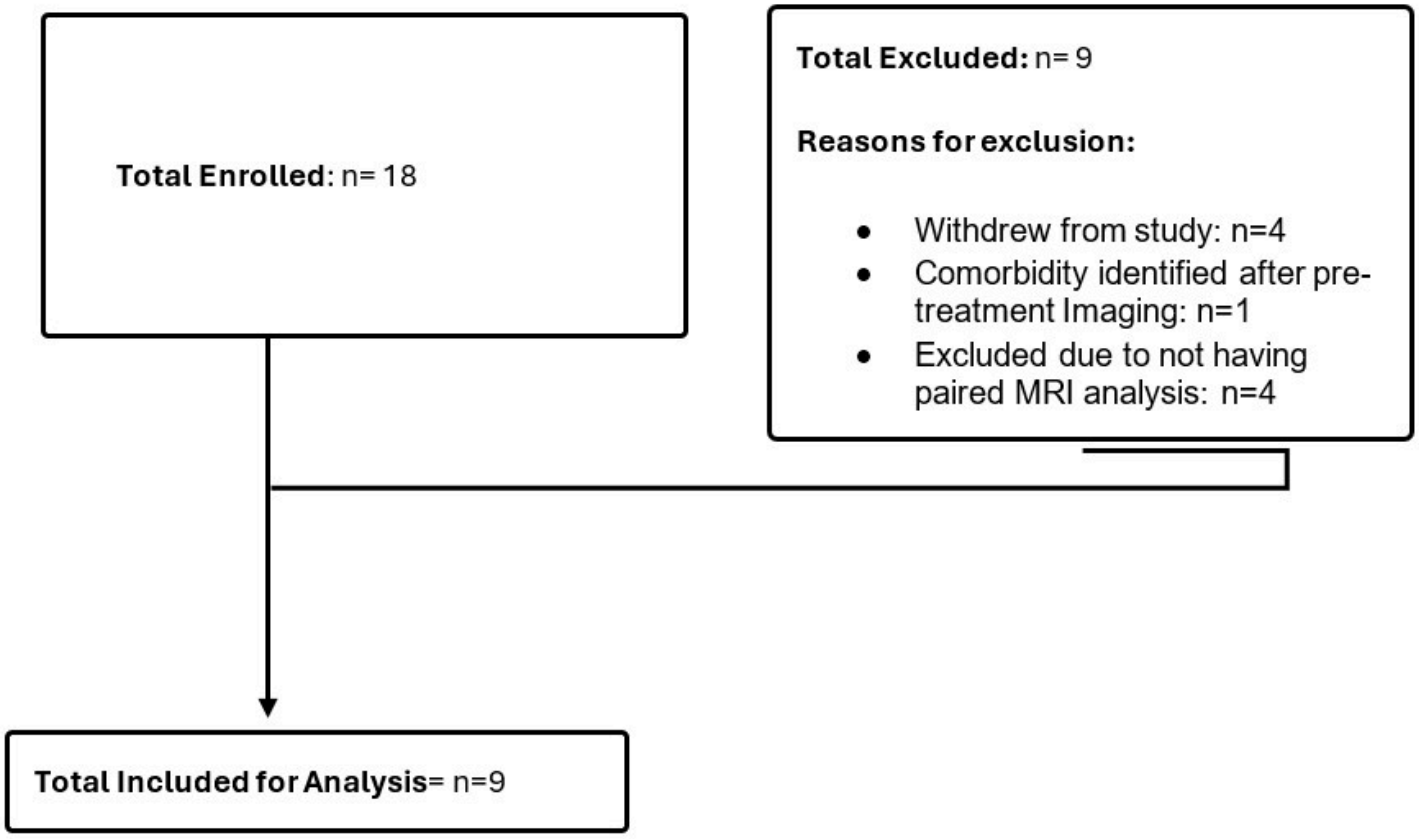


Figure 1

Summary of patient disposition and reasons for exclusion

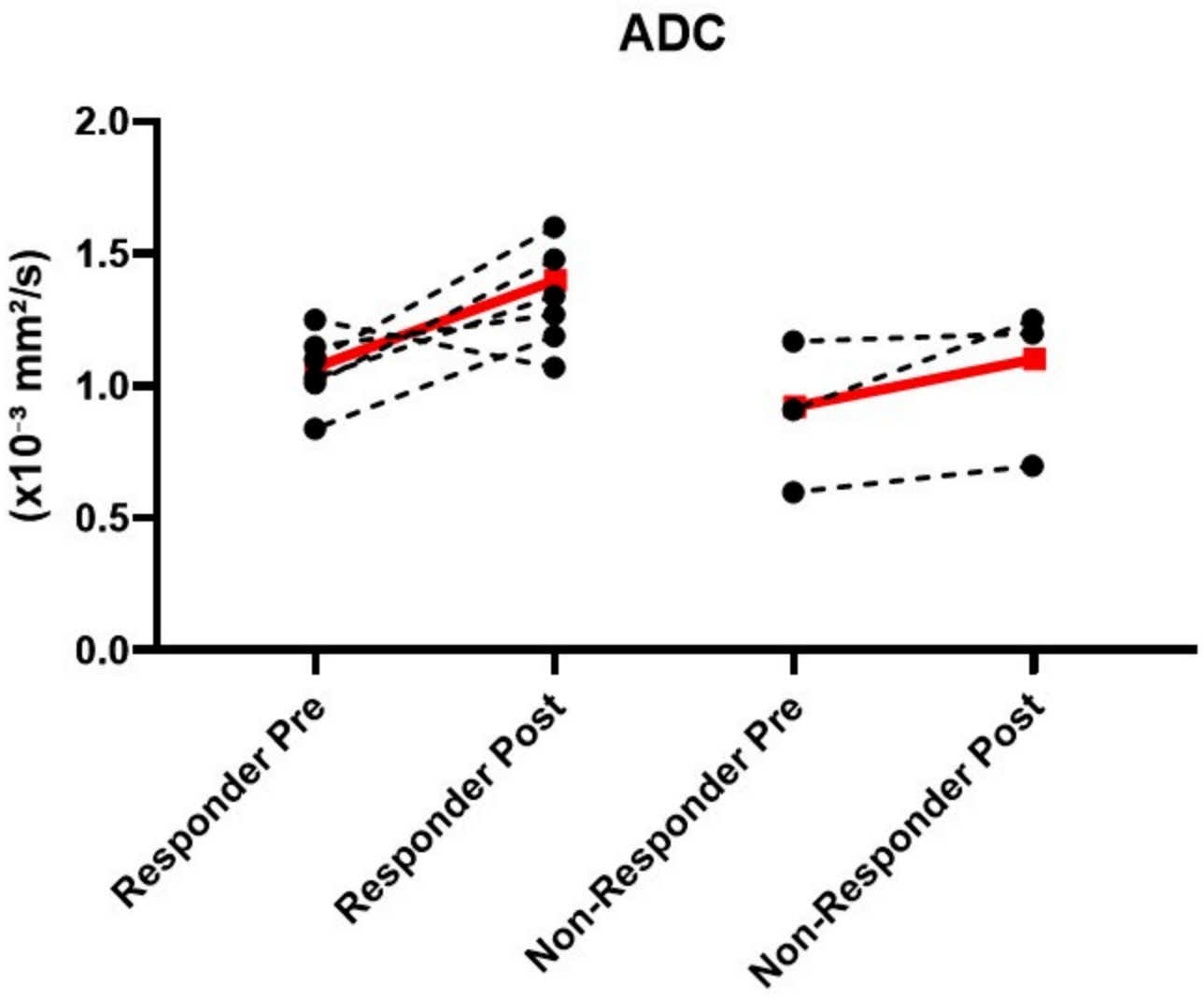


Figure 2

ADC changes pre- and post-treatment in partial responders and non-responders. Black dotted lines show individual trajectories; red lines denote group medians.

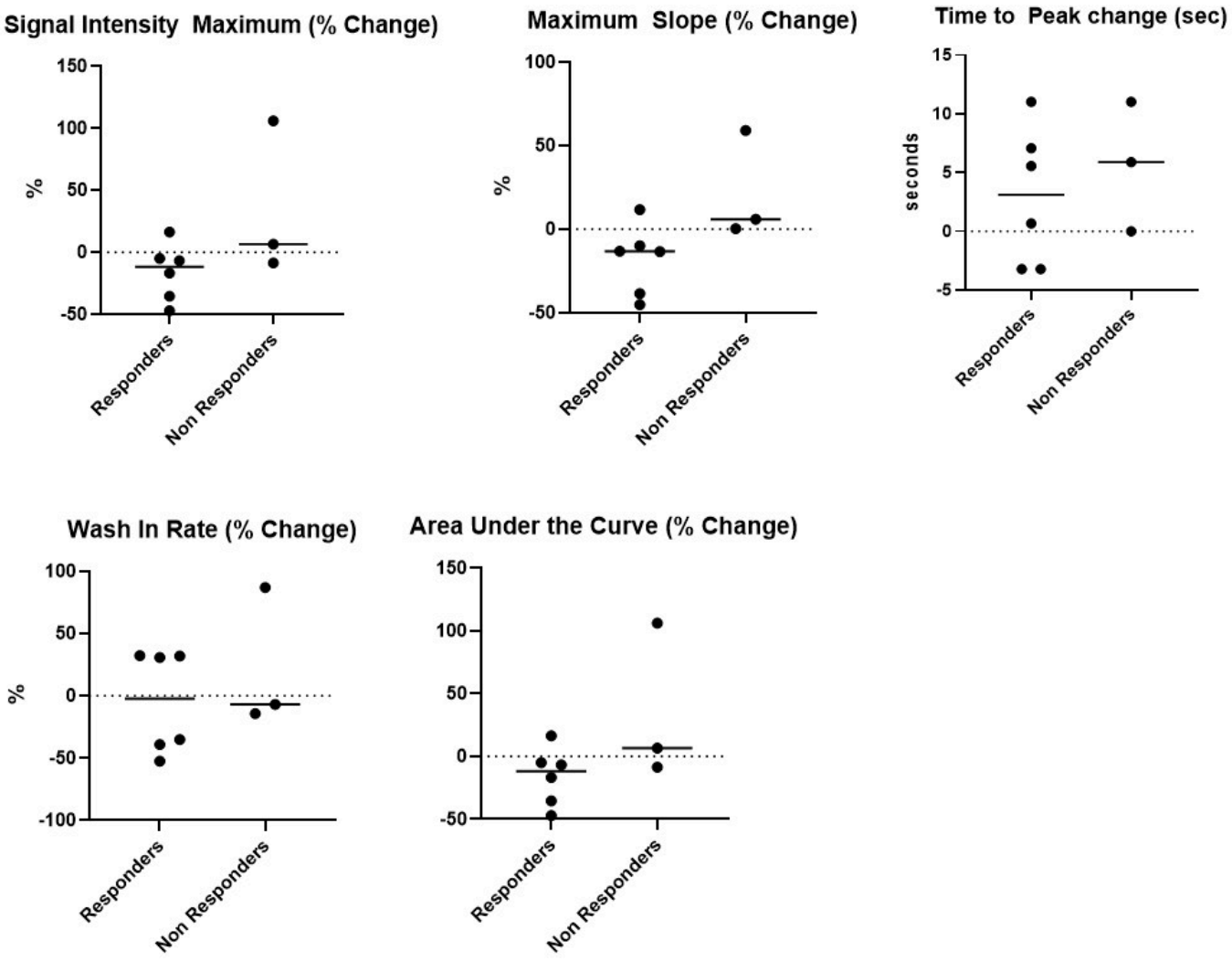


Figure 3

Individual patient percentage change in ultrafast DCE-MRI parameters stratified by pathological response.